Electronic Supplementary Information

An Iridium(III) Complex with Oximated 2,2'-Bipyridine as a Sensitive Phosphorescent Sensor for Hypochlorite

Na Zhao,[†] Yu-Hui Wu,[†] Rui-Min Wang,[†] Lin-Xi Shi,[†] and Zhong-Ning Chen[*,†,‡]

State Key Laboratory of Structural Chemistry, Fujian Institute of Research on the Structure of Matter, Chinese Academy of Sciences, Fuzhou, Fujian 350002, China, and State Key Laboratory of Organometallic Chemistry, Shanghai Institute of Organic Chemistry, Chinese Academy of Sciences, Shanghai 200032, China

Preparation of ROS and RNS

Various ROS and RNS including H_2O_2, ROO·, NO·, $\cdot O_2^-$, ·OH and OCl^- were prepared according to the following methods.[1,2]

The aqueous solutions of H_2O_2 (30%) and NaClO (13%) were purchased form Alfa Aera Chemical Co.

Preparation of ROO·

ROO· was generated from AAPH [2,2'-azobis(2-amidinopropane)dihydrochloride]. 2,2'-Azobis(2-amidinopropane)dihydrochloride (200 μM) in deionizer water was added, then stirred at 25 °C for 30 min.

Preparation of NO·

Nitric oxide was generated from SNP [Sodium Nitroferricyanide (III) Dihydrate]. SNP (final 200 μM) in deionizer water was added then stirred at 25 ^oC for 30 min.

Preparation of $\cdot O_2^-$

$\cdot O_2^-$ was generated by xanthine and xanthine oxidase. Xanthine oxidase was added first. After xanthine oxidase was dissolved, xanthine (final 200 μM) was added and the mixtures were stirred at 25 ^oC for 1 hour.

Preparation of ·OH

Ferrous perchlorate (200 μM) and H_2O_2 (2 mM) were added at room temperature.

References:

1 Z.-N. Sun, F.-Q. Liu, Y. Chen, P. K. H. Tam and D. Yang, *Org. Lett.*, 2008, **10**, 2171;
2 Y.-K. Yang, H. J. Cho, J. Lee, I. Shin and J. Tae, *Org. Lett.*, 2009, **11**, 859.

Table S1. Partial Molecular Orbital Compositions (%) of **1** under the TD-DFT Calculations.

Orbital	Energy (eV)	MO contribution (%)			
		Ir	L1	ppy	
				ppy1	ppy2
LUMO+6	-0.8351	1.2	93.3	2.3	3.2
LUMO+5	-0.8716	5.1	26.7	21.8	46.4
LUMO+3	-1.4569	5.8	3.5	44.2	46.5
LUMO	-2.3481	4.6	92.8	1.4	1.2
HOMO	-5.8070	46.3	3.9	25.0	24.8
HOMO-1	-6.4380	19.8	4.6	37.6	38.0
HOMO-2	-6.5819	57.2	8.2	18.5	16.1
HOMO-3	-6.6843	50.6	13.4	18.1	17.9
HOMO-6	-7.4663	4.4	92.1	1.3	2.2

Table S2. Singlet Absorptions and Triplet Emission Transitions of **1** by the TD-DFT Calculations in DMF Media.

	Transition	**Contri.**	***E*, nm (eV)**	**O.S.**	**Assignment**
T1	HOMO→LUMO	94.7%	587 (2.11)	0.0000	^{3}MLCT /^{3}LLCT
S1	HOMO→LUMO	100%	472 (2.63)	0.0010	^{1}MLCT /^{1}LLCT
S5	HOMO-1→LUMO	70.0%	368 (3.37)	0.1021	^{1}MLCT /^{1}LLCT
	HOMO→LUMO+3	14.9%			^{1}MLCT /^{1}ILCT
S21	HOMO-6→LUMO	65.2%	289 (4.29)	0.2855	^{1}ILCT
	HOMO-3→LUMO+3	9.0%			^{1}MLCT /^{1}LLCT/^{1}ILCT
S36	HOMO-2→LUMO+5	33.8%	256 (4.83)	0.3715	^{1}MLCT/^{1}ILCT
	HOMO-1→LUMO+6	30.6%			^{1}MLCT/^{1}LLCT

Table S3. Partial Molecular Orbital Compositions (%) of **2** under the TD-DFT Calculations.

Orbital	Energy (eV)	MO contribution (%)			
		Ir	L2	ppy	
				ppy1	ppy2
LUMO+6	-0.8580	4.7	2.1	55.5	37.7
LUMO+5	-0.9045	5.1	22.9	26.0	46.0
LUMO+2	-1.5834	5.0	3.7	44.7	46.6
LUMO+1	-1.8126	1.2	94.1	2.2	2.5
LUMO	-2.5786	4.9	92.4	1.5	1.2
HOMO	-5.8513	45.7	3.9	25.4	25.0
HOMO-1	-6.4726	14.2	2.9	41.9	41.0
HOMO-2	-6.6453	51.1	4.4	21.4	23.1
HOMO-3	-6.7779	51.6	8.5	17.9	22.1
HOMO-6	-7.5831	1.1	97.5	0.7	0.7

Table S4. Singlet Absorptions and Triplet Emission Transitions of **2** by the TD-DFT Calculations in DMF Media.

	Transition	**Contri.**	***E*, nm (eV)**	**O.S.**	**Assignment**
T1	HOMO→LUMO	100%	641 (1.93)	0.0000	^{3}MLCT /3LLCT
S1	HOMO→LUMO	100%	510 (2.43)	0.0009	^{1}MLCT /1LLCT
S5	HOMO→LUMO+2	91.6%	375 (3.30)	0.0626	^{1}MLCT /1LLCT
S20	HOMO-6→LUMO	57.3%	290 (4.27)	0.2430	^{1}ILCT
	HOMO-3→LUMO+1	30.7%			^{1}MLCT /1LLCT
S37	HOMO-2→LUMO+5	36.5%	255 (4.86)	0.4202	^{1}MLCT/1ILCT/1LLCT
	HOMO-1→LUMO+6	31.3%			^{1}ILCT

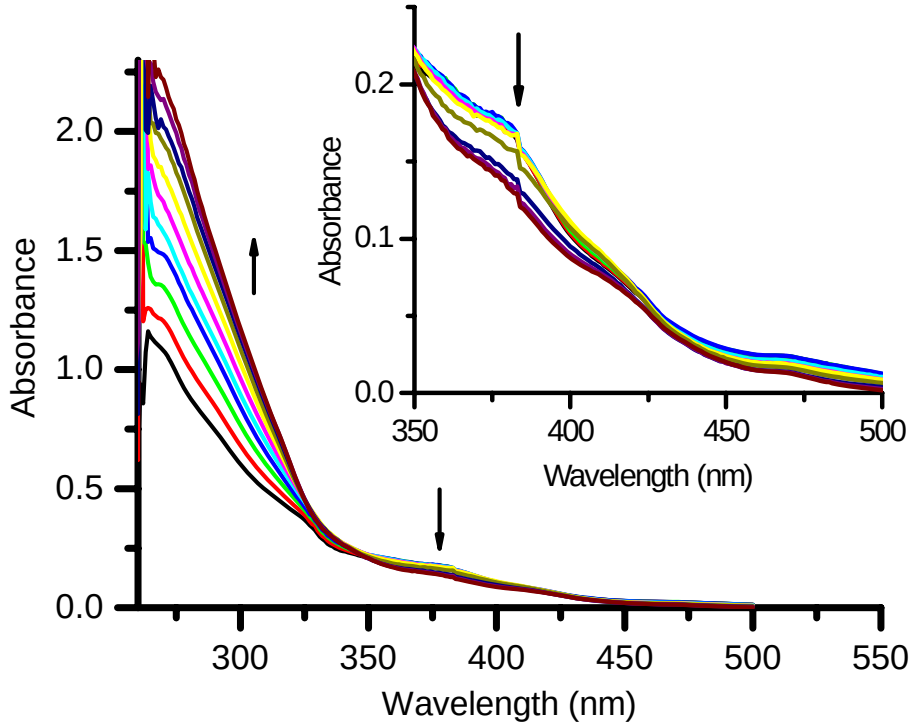

Fig. S1 The change of UV−vis spectra of complex **1** with ClO^- in DMF−HEPES (50 mM, pH 7.2, v/v, 4:1).

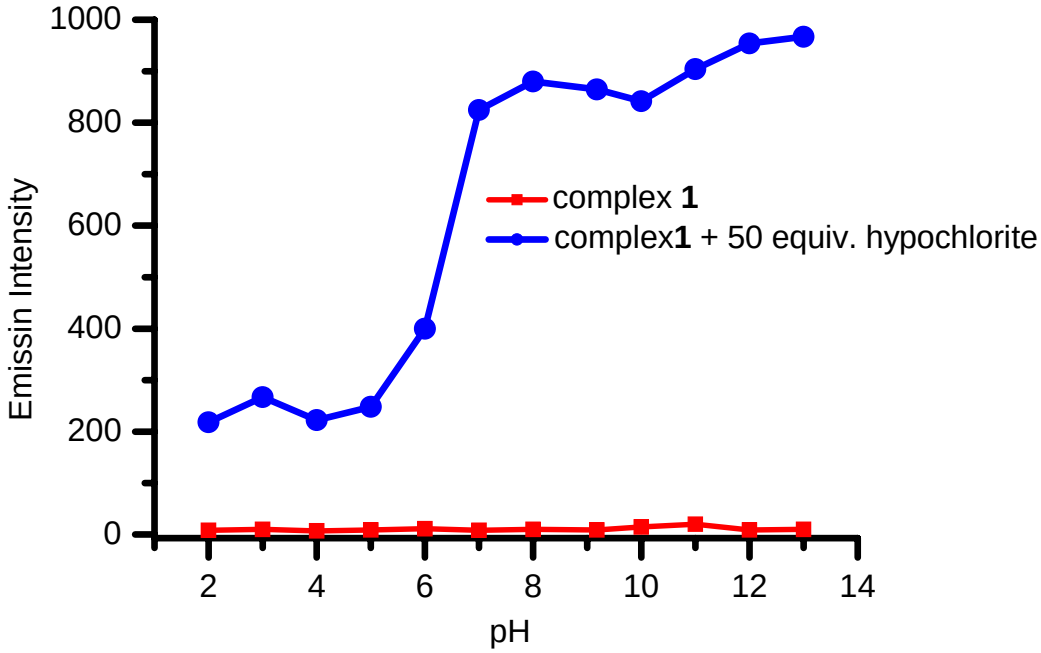

Fig. S2 The emission intensity of complex **1** (20 μM) at 587 nm in the absence (■) and presence (●) of 50 equiv. ClO^- at various pH values.

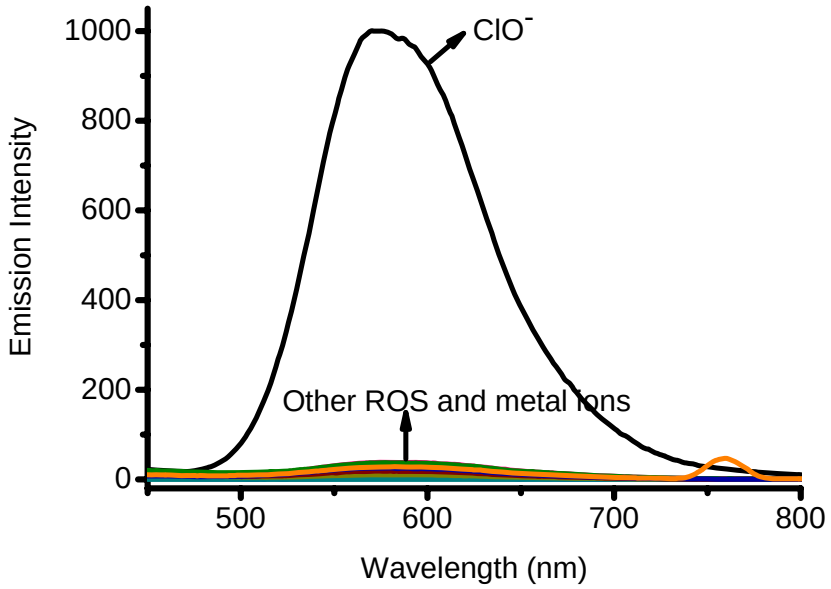

Fig. S3 the emission spectra of complex **1** (20 μM) in CH_3CN in response to ROS and other metal ions.

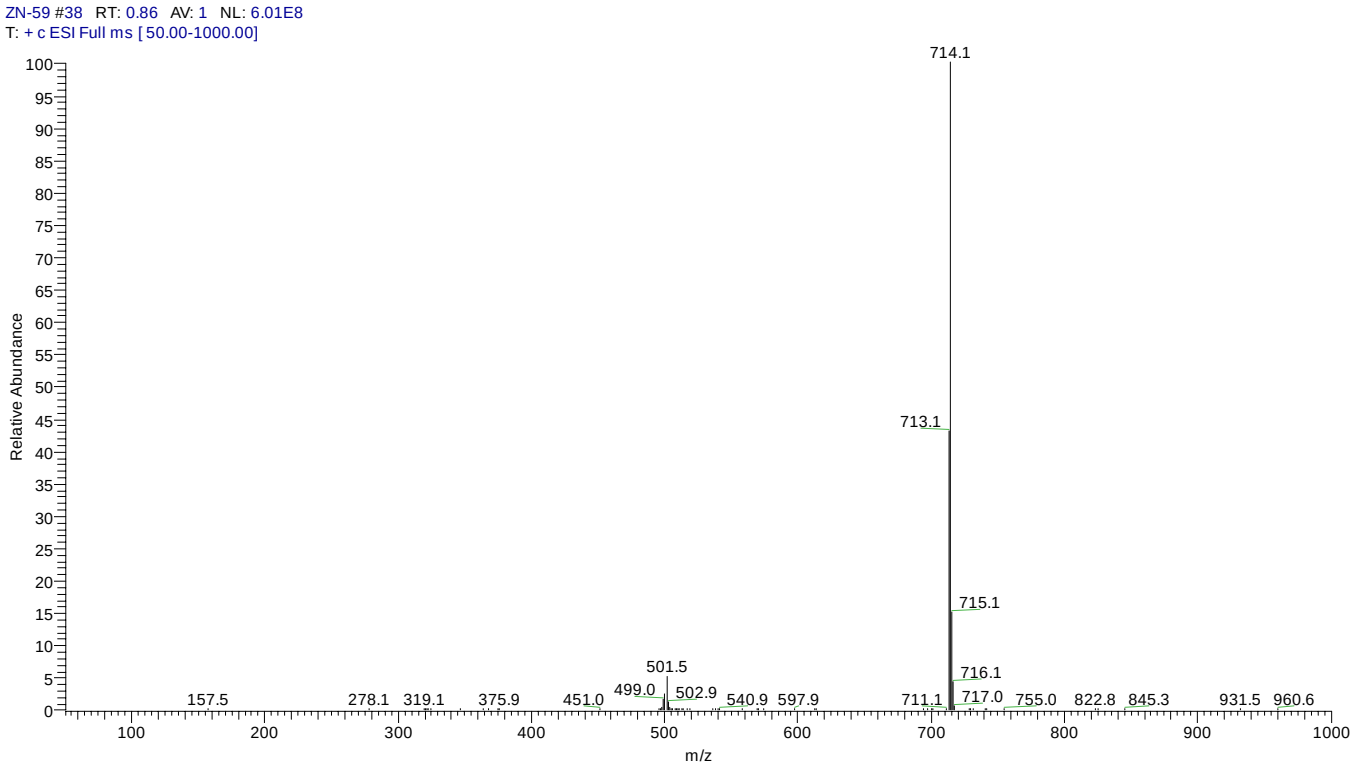

(a)

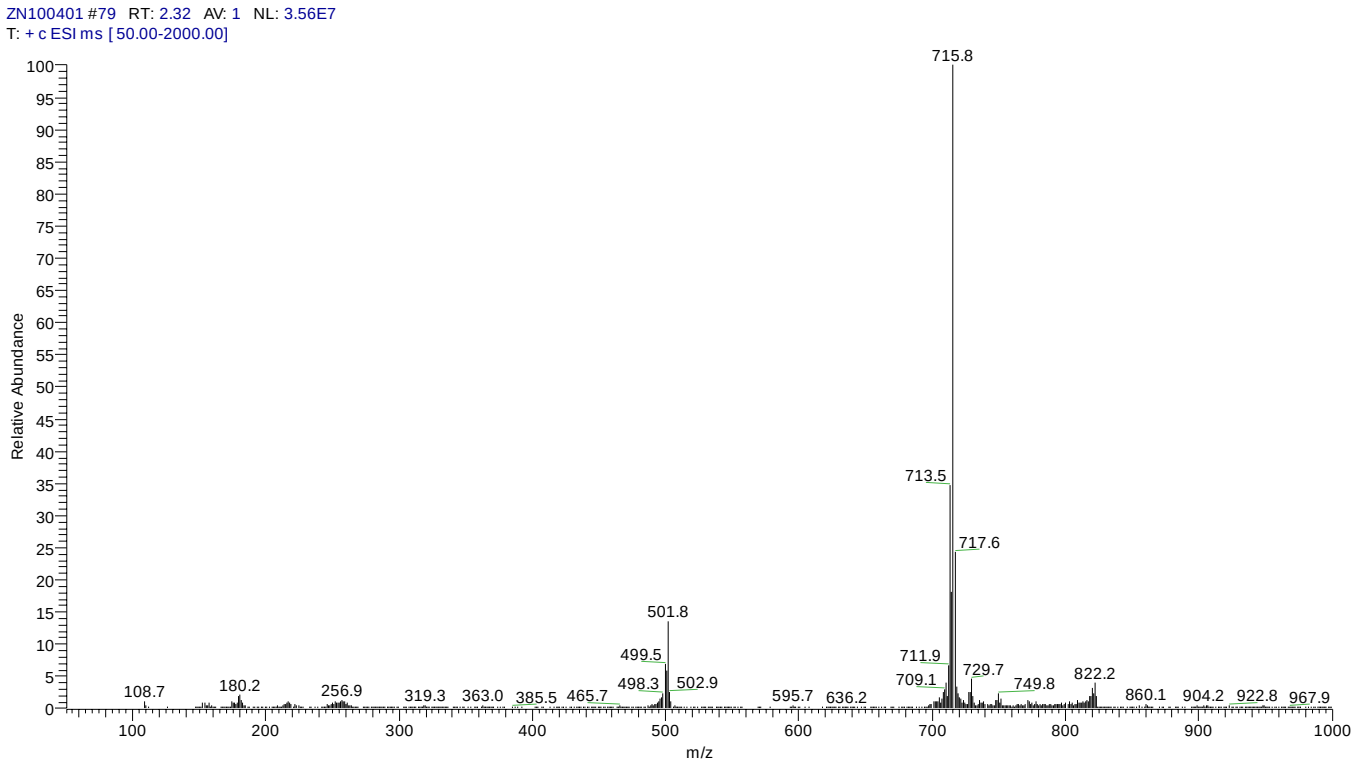

(b)

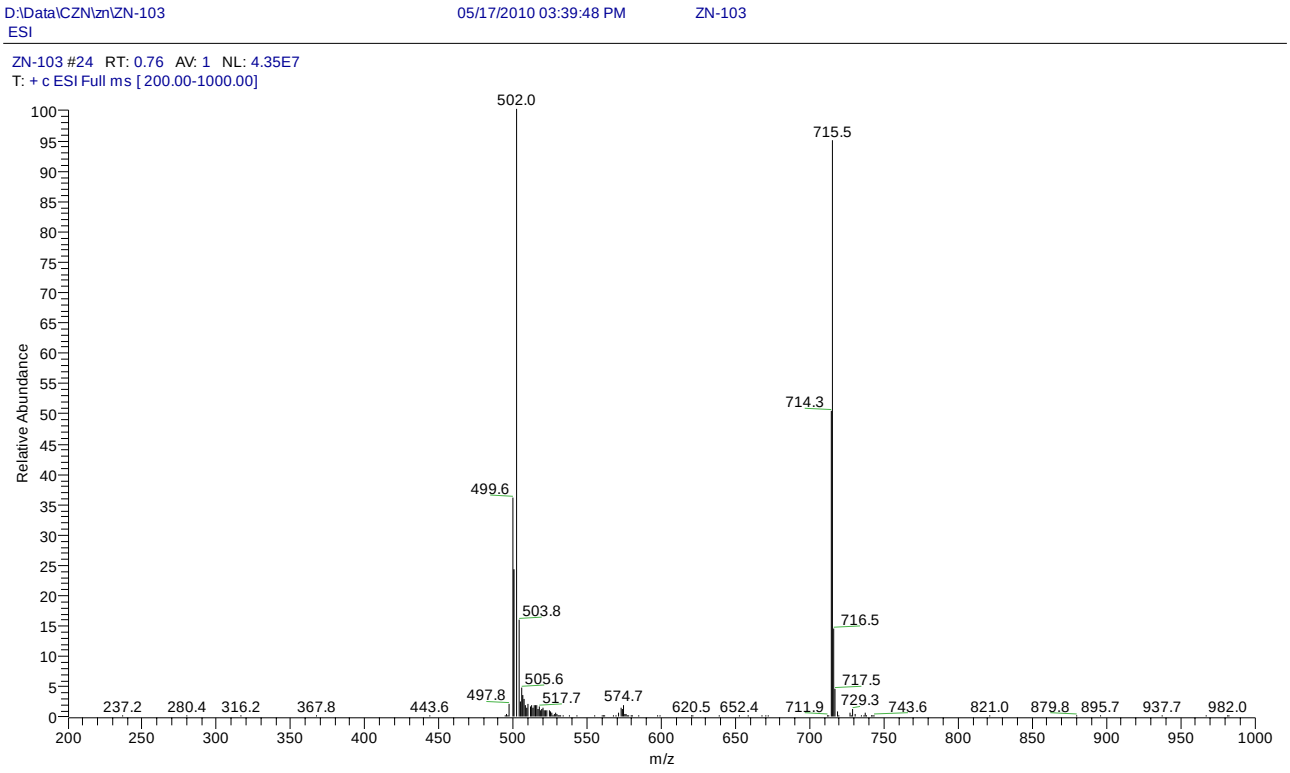

(c)

Fig. S4 Positive ion ESI-MS. (a) complex **1**, (b) the isolated product of **1** with ClO^-, (c) complex **2.**

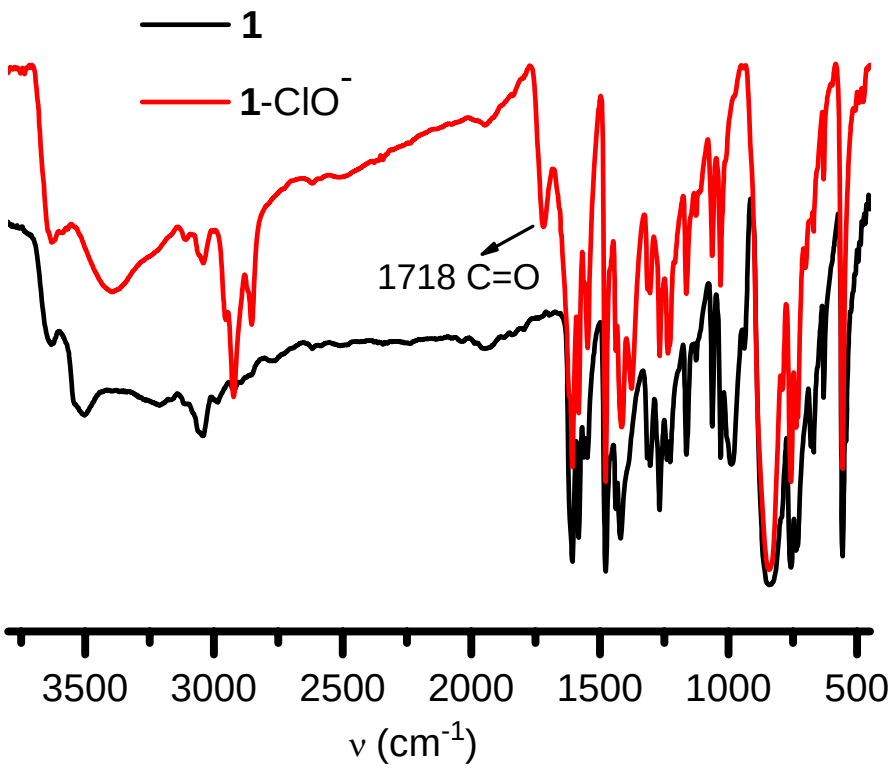

Fig. S5 The IR spectra of complex **1** and the isolated product of **1** with ClO^-.

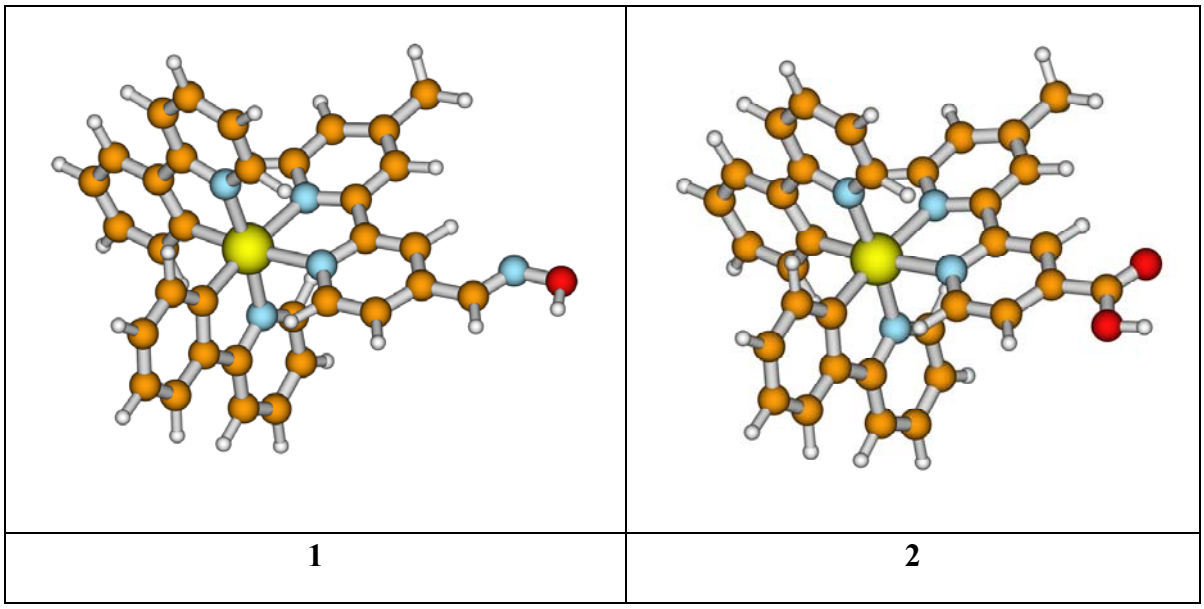

Fig. S6 Optimized structure of **1** and **2** in the ground state with DFT method at the PBE1PBE level.

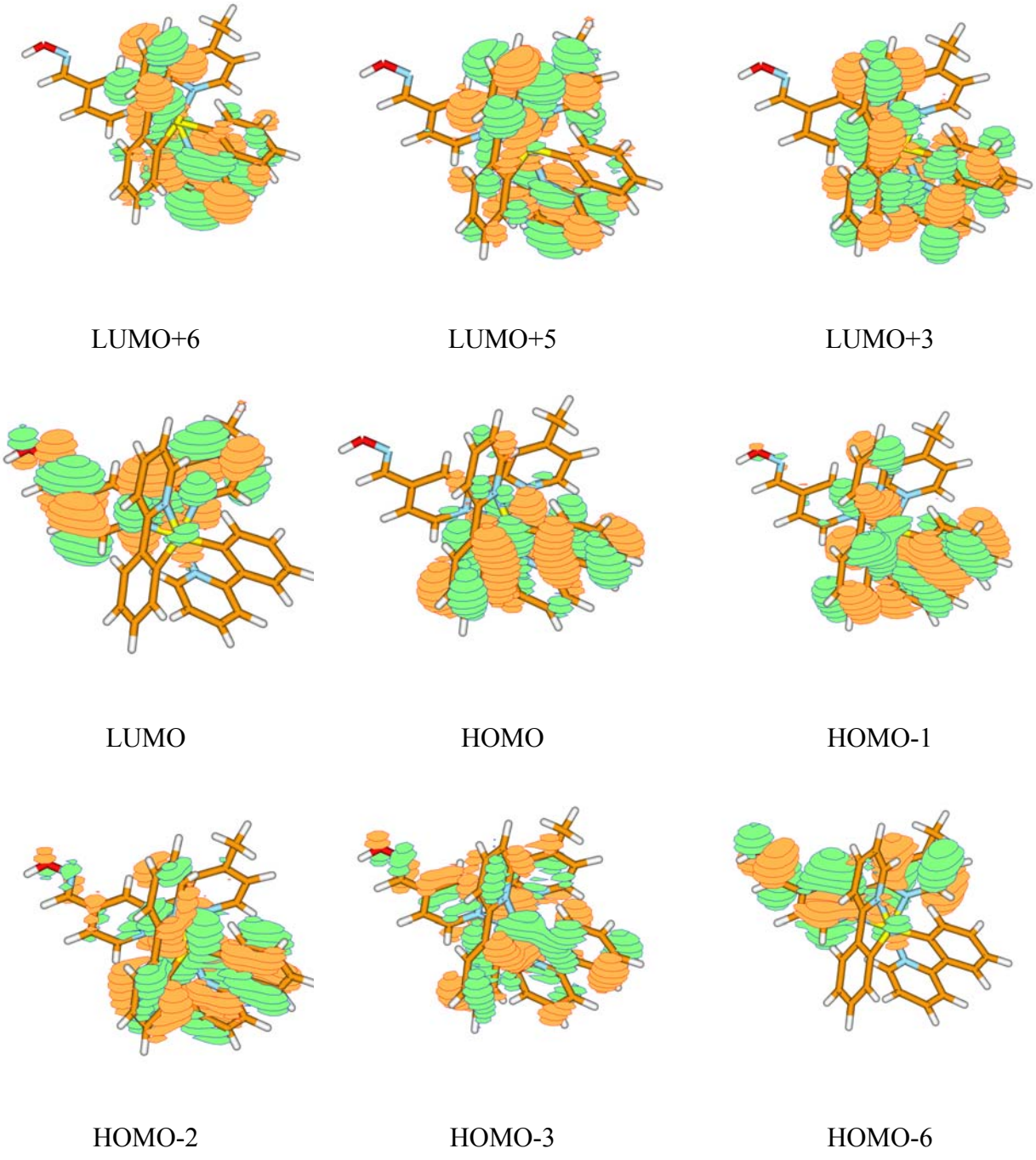

Fig. S7 Electron-density diagrams of the frontier molecular orbitals involved in the absorption of (*E*)**-1** in DMF solution.

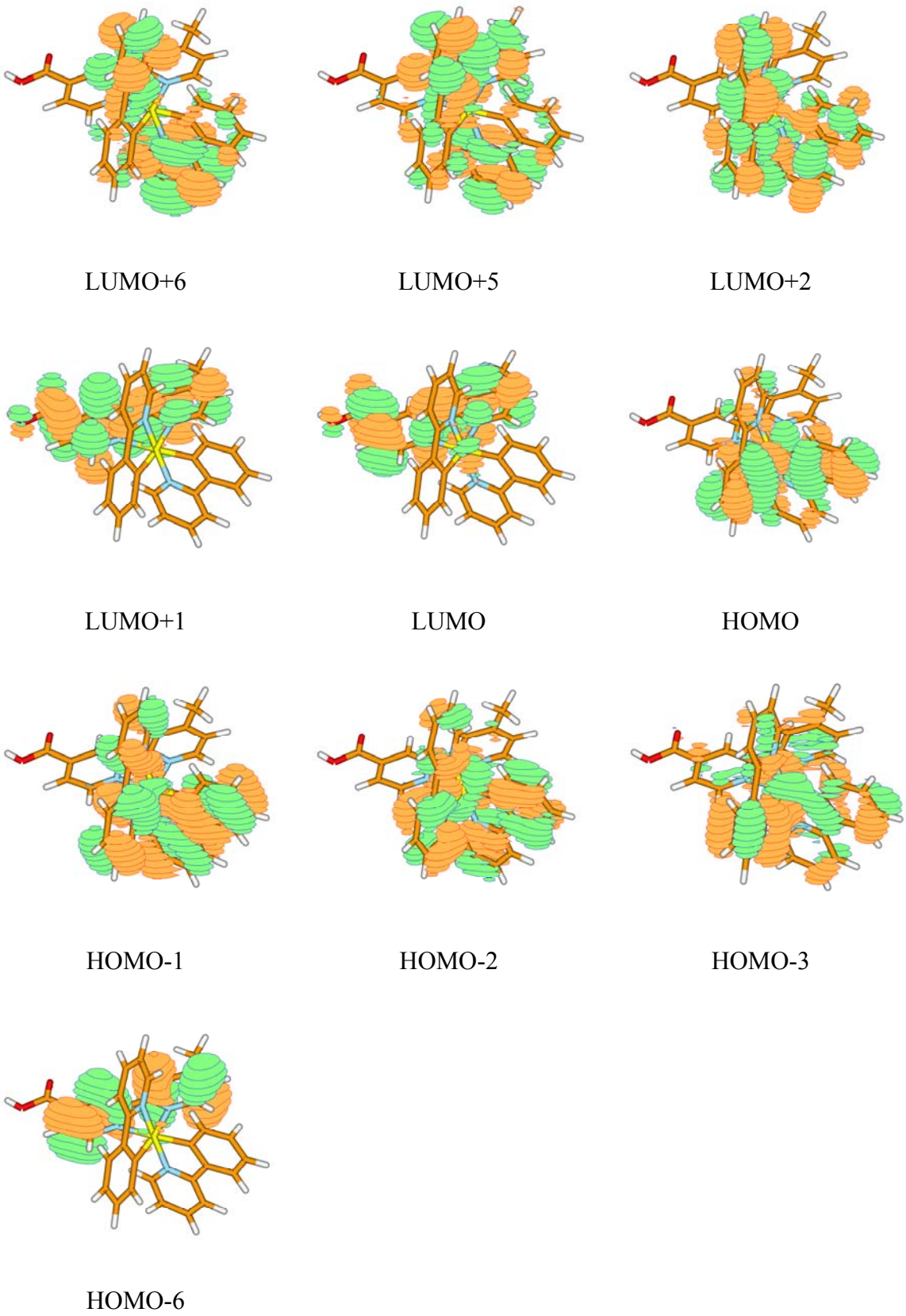

Fig. S9 Electron-density diagrams of the frontier molecular orbitals involved in the absorption of **2** in DMF solution.